Analytic treatment of the precessional (ballistic) contribution to the conventional magnetic switching

Ya. B. Bazaliy[1,2,*]

[1]*Department of Physics and Astronomy, University of South Carolina, Columbia, SC 29208, USA*
[2]*Institute of Magnetism, National Academy of Science, Kyiv 03142, Ukraine*

(Dated: June 21, 2011)

We consider a switching of the magnetic moment with an easy axis anisotropy from an "up" to a "down" direction under the influence of an external magnetic field. The driving field is applied parallel to the easy axis and is continuously swept from a positive to a negative value. In addition, a small constant perpendicular bias field is present. It is shown that while the driving field switches the moment in a conventional way, the perpendicular field creates an admixture of the precessional (ballistic) switching that speeds up the switching process. Precessional contribution produces a non-monotonic dependence of the switching time on the field sweep time with a minimum at a particular sweep time value. We derive an analytic expressions for the optimal point, and for the entire dependence of the switching time on the field sweep time. Our approximation is valid in a wide parameter range and can be used to engineer and optimize of the magnetic memory devices.

I. INTRODUCTION

Conventional magnetic switching by an externally applied magnetic field $\mathbf{H}$ is the basis of magnetic recording in hard disk drives and other devices. The speed at which the moments of the magnetic bits can be switched between the two easy directions has obvious implication for the technology performance, setting the limit for the information writing rate. In general, the magnetic switching time τ_m depends on the material parameters, sample size and shape. Here we are interested in the dependence of τ_m on the rate of change of the driving magnetic field. We will call the time τ_h required to flip the external magnetic field a "field sweep time". This time is of course finite in any real device used for magnetic writing. Clearly, very long field sweep times will make the magnetic switching very slow. One can argue then that, since τ_m will decrease with decreasing τ_h, the best case scenario for switching is the instantaneous flip of the external field with $\tau_h = 0$. However, it was found numerically[1] that in realistic conditions the function $\tau_m(\tau_h)$ is not monotonic and has a minimum at a particular value of the sweep time τ_h^*. The field sweep time corresponding to this minimum is optimal and any further decrease of τ_h will be counterproductive in terms of the technology performance. An analytic expression for $\tau_m(\tau_h)$ was announced in Ref. 2. That paper also explained the physical reason behind the existence of the switching time minimum. In the present paper we provide the detailed derivation of the approximate analytic expressions for the function $\tau_m(\tau_h)$ and the optimal field sweep time τ_h^*. We then discuss the limits of their validity and compare analytic approximations with the exact numeric results.

Before proceeding to the derivations, we would like to place the phenomenon under investigation into context. Magnetic switching and its speed are important technological parameters and were studied by many authors. We will concentrate on a single-domain magnet described by a moment $\mathbf{M}$ with an easy axis anisotropy energy. Its switching under a static applied field is described by the Stoner-Wholfarth astroid[3] in the H-space (Fig. 1, $\hat{z}$ is pointing along the easy axis). If the applied field is changed infinitesimally slowly, and the thermal fluctuations of the moment can be neglected, magnetic switching is achieved when the trajectory of the driving field in the H-space crosses the astroid boundary. The switching process begins at the moment of crossing and requires a finite time that depends on the crossing point.

If the magnitude and the direction of the applied field are allowed to change during the magnetic switching process, the number of switching scenarios becomes infinite. In the most general case one wants to optimize the dependence $\mathbf{H}(t)$ so as to minimize the switching time. Different minimization schemes are discussed theoretically,[4–6] but their experimental realization is distant as they all require external fields that change exceedingly rapidly and have carefully controlled magnitude and direction.

A large body of research is devoted to a restricted case of pulsed applied fields with fixed direction. The easiest pulse shape to produce experimentally is a field jump from an initial value $\mathbf{H}_i$ to a final value $\mathbf{H}_f$. The jump can be instantaneous (step function) or have a certain rise time (smeared step function). After the jump the field stays at the final value $\mathbf{H}_f$. The equilibrium directions of the moment before and after the jump are described by the Stoner-Wohlfarth picture with $\mathbf{H} = \mathbf{H}_i$ and $\mathbf{H} = \mathbf{H}_f$ respectively. Before the field jump the moment resides in the minimum $\mathbf{M}_i$ of the magnetic energy corresponding to the initial field. After the field jump the moment eventually reaches the equilibrium $\mathbf{M}_f$, corresponding to the minimum of the energy at the final external field. (We will consider situations where the energy has only one minimum). The switching time depends on both the initial and final directions of the moment or, equivalently, on both $\mathbf{H}_i$ and $\mathbf{H}_f$.[7] This leads to some interesting properties even for the idealized case of an instantaneous jump. For example, switching below the

Stoner-Wholfarth limit becomes possible,[8–11] and is accompanied by interesting counter-intuitive phenomena. The usual property of switching time to decrease with with the increasing magnitude of H_f, observed for $\mathbf{H}_f$ outside of the astroid, may reverse when $\mathbf{H}_f$ is inside the astroid.[12]

If instead of the field jumps one uses pulses with the field switched from zero to a fixed value for a finite time period, more options for switching time minimization become available. In the absence of magnetic anisotropy the fastest 180° flip of a moment is achieved by applying the field $\mathbf{H}$ perpendicular to $\mathbf{M}_i$. The field is turned on, and the moment starts to precess around $\mathbf{H}$. After a half of the precession period it reaches the direction $\mathbf{M}_f = -\mathbf{M}_i$, at which time the field has to be switched off. This scheme constitutes the simplest example of "precessional" or "ballistic" switching. In the presence of anisotropy precessional switching becomes more complicated, but is still possible.[13–17] The key ingredients of the precessional switching are extremely short pulses of precise duration and sufficiently strong field magnitude. Ideally their rise and fall times should approach zero, but this is very hard to achieve experimentally as the pulse duration should be of the order of picoseconds. Precessional switching was observed using the fields created by pulses of synchrotron radiation[18] or by a careful pulse shaping using femtosecond lasers,[19] but is not yet used in applications. The speed of the precessional switching increases with the field magnitude, but cannot be increased infinitely due to the breakdown of the ferromagnetic state of the sample.[20]

Another widely discussed class of switching scenarios is the application of the high-frequency oscillating field, or an RF-signal. When the frequency of the RF signal is close to the eigenfrequency of the magnetic moment, a magnetic resonance occurs and a continuous precession state is established. The amplitude of the precession is growing as the strength of the RF signal is increased. Sufficiently large signal would in principle be able to increase the amplitude so much as to switch the magnetization from "up" to "down". Experiments observed an RF-assisted switching[21] happening inside the Stoner-Wohlfarth astroid. In this case the RF signal helps the external field to drive the transition. To improve the RF-assisted switching the schemes with variable ("chirped") frequency are designed theoretically.[22–27] Their goal is to keep the frequency equal to the instantaneous, amplitude-dependent resonance frequency of the magnet. Various instabilities may prevent the purely RF switching by destroying the coherent single-domain state of a sample. However, they are supposed to be suppressed in the magnetic particles with the sizes below $10 \div 20$ nm.[12,25]

The phenomenon considered in the present paper is different from all of the above. We consider conventional switching by a field jump, but concentrate on the switching time τ_m dependence on the jump rise time τ_h. The function $\tau_m(\tau_h)$ exhibits an unexpected minimum which was not discussed in the literature. As it will be shown in the conclusions, the minimum of $\tau_m(\tau_h)$ results from an admixture of a precessional (ballistic) switching to the conventional switching, an effect which can be named a ballistic-assisted switching. Normally, the ballistic contribution of a small perpendicular field is quenched by the large anisotropy, but here it is restored by the time-dependence of the switching field during the rise time of the jump. This type of ballistic contribution can be observed for infinitesimally small perpendicular fields, which distinguishes it is from the purely ballistic case where a finite field comparable to the anisotropy fields is required. Our analysis also shows that the phenomena of ballistic-assisted and RF-assisted switching are complimentary. Both can be treated on equal footing by considering the averaging of the perturbation field torque during the precession cycle of the moment in the strong anisotropy field.

II. MODEL

Our treatment is based on the Landau-Lifshitz equation, and does not take into account thermal fluctuations. We consider a single domain magnetic bit described by a magnetic moment $\mathbf{M} = M_0\mathbf{n}$, where $\mathbf{n}$ is a unit vector. The magnet has an easy anisotropy axis directed along z, and its anisotropy energy is given by $E_a = -(1/2)Kn_z^2$. This anisotropy creates two equilibrium directions of the moment along $+z$ and $-z$.

The switching field $\mathbf{H} = H(t)\hat{z}$ is directed along z as well. It favors the $+z$ direction for $H > 0$ and $-z$ for $H < 0$. For large enough magnitudes, $|H| > K/M_0$, there is no equilibrium in the direction opposite to the field.

When the external field is pointing along the easy axis direction, magnetic switching relies on the fluctuations near the equilibrium position. Without them a moment pointing exactly along $+z$ will not be switched by any amount of negative applied field. Instead it will remain at the point of unstable equilibrium, until an initial fluctuation occurs and then grows with time. The switching time in this case strongly depends on the fluctuation magnitude $\delta\theta$, being infinite for $\delta\theta = 0$.[28,29] In order to model the required initial fluctuation we apply a small bias field $\mathbf{H}_\perp = H_\perp\hat{x}$ perpendicular to the easy axis. This field is set to be constant in time. It creates a controlled deviation of the initial magnetization from the field direction and makes the problem well defined.

The switching dynamics is described by the Landau-Lifshitz-Gilbert (LLG) equation.

$$\dot{\mathbf{M}} = -\gamma\left[\frac{\partial E}{\partial \mathbf{M}} \times \mathbf{M}\right] + \frac{\alpha}{M_0}[\mathbf{M} \times \dot{\mathbf{M}}] \ ,$$

where γ is the gyromagnetic ratio, $E = E_a - (\mathbf{H}+\mathbf{H}_\perp)\cdot\mathbf{M}$ is the magnetic energy, and α is the Gilbert damping

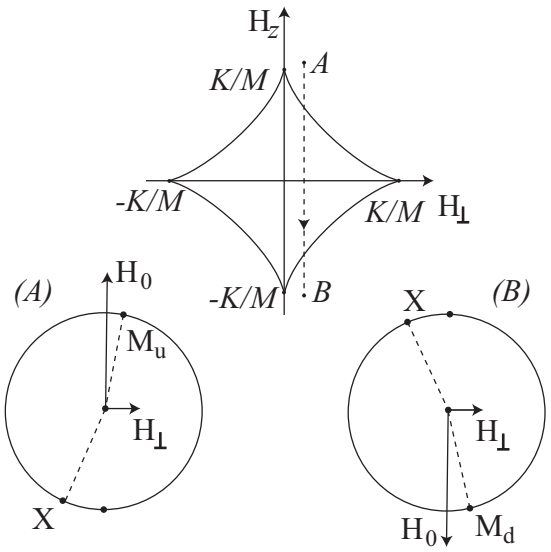

FIG. 1: Top: Stoner-Wohlfarth astroid in the H-space and the trajectory of the magnetic field change (dashed line) during the rise time of the pulse with axial field sweep from $+H_0$ to $-H_0$ at a constant perpendicular bias $H_\perp$. The lower panels (A) and (B) correspond to the initial and final directions of the field. They show the "up" and "down" minimum points M_u, M_d, and maximum points X of the magnetic energy.

constant. In terms of the unit vector $\mathbf{n}$ it reads

$$\dot{\mathbf{n}} = -\left[\frac{\partial\varepsilon}{\partial\mathbf{n}} \times \mathbf{n}\right] + \alpha[\mathbf{n} \times \dot{\mathbf{n}}] \tag{1}$$

with $\varepsilon = \gamma E/M_0$. Using the spherical angles (θ, ϕ), defined so that $\mathbf{n} = \{n_x, n_y, n_z\} = \{\sin\theta\cos\phi, \sin\theta\sin\phi, \cos\theta\}$, one gets a system of equations

$$(1+\alpha^2)\dot{\theta} = -\frac{1}{\sin\theta}\frac{\partial\varepsilon}{\partial\phi} - \alpha\frac{\partial\varepsilon}{\partial\theta}\ , \tag{2}$$

$$(1+\alpha^2)\dot{\phi} = \frac{1}{\sin\theta}\frac{\partial\varepsilon}{\partial\theta} - \frac{\alpha}{\sin^2\theta}\frac{\partial\varepsilon}{\partial\phi}\ . \tag{3}$$

Actual materials are characterized by $\alpha \ll 1$ and we will always calculate up to the linear terms in α, e.g., $1+\alpha^2 \approx 1$. In our case the energy has the form

$$\begin{aligned}\varepsilon(\theta,\phi) &= -\frac{\omega_0}{2}n_z^2 - h(t)n_z - h_\perp n_x = \\ &= -\frac{\omega_0}{2}\cos^2\theta - h(t)\cos\theta - h_\perp\sin\theta\cos\phi\ ,\end{aligned} \tag{4}$$

where $\omega_0 = \gamma K/M_0$, $h = \gamma H$, $h_\perp = \gamma H_\perp$. The smallness of the bias field is ensured by the condition $h_\perp \ll \omega_0$.

The field sweep is assumed to be linear in time and given by the expressions

$$\begin{aligned}h(t) &= +h_0\ , \quad (t<0)\\ h(t) &= h_0\left(1-\frac{2t}{\tau_h}\right)\ , \quad (0<t<\tau_h)\\ h(t) &= -h_0\ , \quad (t>\tau_h)\ .\end{aligned} \tag{5}$$

The trajectory of the magnetic field change and the positions of the minima and maxima of the magnetic energy for the initial and final field orientations are shown in Fig. 1. We start with the positive field $h = +h_0 > \omega_0$ which guarantees that the magnet is initially pointing close to the $+z$ direction. This state will be called an "up-equilibrium". At the end of the reversal the moment reaches the "down-equilibrium", corresponding to $h = -h_0$. The initial and final directions of the moment are determined from the conditions $\partial\varepsilon/\partial\phi = 0$, $\partial\varepsilon/\partial\theta = 0$ with $h = \pm h_0$. This gives $\phi = 0$ and an equation for θ reading

$$\omega_0\sin\theta\cos\theta \pm h_0\sin\theta - h_\perp\cos\theta = 0\ .$$

In the limit $h_\perp \ll \omega_0$ one finds the following approximations for the values of the polar angles in the up- and down-equilibria

$$\theta_u \approx \frac{h_\perp}{\omega_0 + h_0}\ , \quad \theta_d \approx \pi - \frac{h_\perp}{\omega_0 + h_0}\ . \tag{6}$$

As the field is swept from positive to negative values, the up-equilibrium disappears and the magnetic moment starts to move in a spiral fashion towards the down-equilibrium, approaching it exponentially. To define a finite switching time we have to introduce a provisional cut-off angle θ_{sw} and calculate the time it takes to reach θ_{sw} during the switching process. The remaining distance from θ_{sw} to θ_d takes extra time, but this time interval does not depend on the field sweep time since in the regimes studied in our paper $\tau_h < \tau_m$, and the remaining motion happens at a constant external field. We use the commonly adopted[1,8,10,12] value of $\theta_{sw} = \pi/2$.

III. NUMERIC RESULTS: NON-MONOTONIC DEPENDENCE OF THE SWITCHING TIME

The LLG equation can be easily solved numerically and the switching time dependence $\tau_m(\tau_h)$ can be obtained. Fig. 2 shows the results of such modeling for a particular parameter set (see figure caption). The minimum of τ_m is clearly observed.

We will show in the subsequent sections that the switching time can be approximated by an expression

$$\tau_m = \frac{3h_0+\omega_0}{4h_0}\tau_h + \frac{\ln[h_0/\pi h_\perp^2\tau_h]}{2\alpha(h_0-\omega_0)} + \tau_R(\alpha, h_0, \omega_0)$$

where τ_R is independent of τ_h and $h_\perp$. As one can see in Fig. 2 the correspondence between the actual (numeric) and approximate curves is quite good and reproduces the minimum of τ_m.

A note on the numeric calculation is due here. It is more convenient to follow the time dependence of the total energy $\varepsilon(t)$, than that of $\theta(t)$. The reason for that is as follows. In the regime considered here the switching time and field sweep time satisfy $\tau_m > \tau_h$ and the switching threshold $\theta = \pi/2$ is reached when the external field

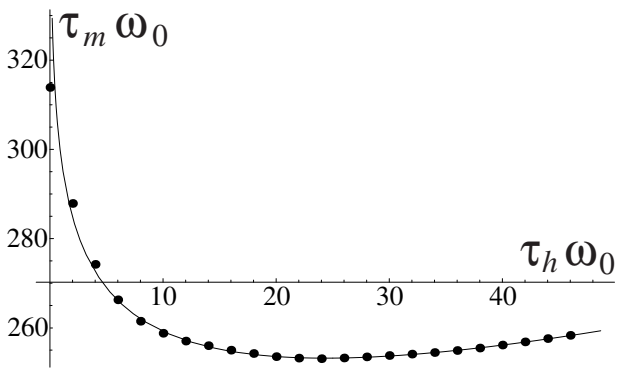

FIG. 2: Switching time as a function of field sweep time (time is measured int he units of ω_0^{-1}). Parameter values are $\alpha = 0.01$, $h_0 = 3.5\ \omega_0$, $h_\perp = 0.001\ \omega_0$. The thin solid line is the approximate expression derived in this paper.

is already time-independent, $h = -h_0$. According to the LLG equation, at constant external field the time derivative of energy is strictly negative

$$\dot{\varepsilon}(t) = -\alpha \dot{\mathbf{n}}^2 < 0 \ ,$$

and $\varepsilon(t)$ is a strictly decreasing function of time. This property greatly simplifies the solution of the equation $\varepsilon(\tau_m) = \varepsilon_{sw}$, where ε_{sw} is the new cut-off, introduced instead of θ_{sw}. Note that in contrast to $\varepsilon(t)$ the time dependence of $\theta(t)$ is non-monotonic. One can easily understand that by recalling that in the $\alpha \ll 1$ limit the spiral motion of the moment approximately follows the equipotential lines. Due to the presence of the bias field $h_\perp$ the latter differ from the $\theta = \text{const}$ lines, leading to the oscillations of $\theta(t)$ in time. In other words, the fact that $\varepsilon(\theta, \phi)$ depends on both spherical angles makes the cut-offs θ_{sw} and ε_{sw} not completely equivalent. Nevertheless, they serve the same purpose with the latter being a more convenient choice. We adopt the cut-off value $\varepsilon_{sw} = \varepsilon(\pi/2, \pi/2) = 0$, closest to the original definition.[1]

IV. ANALYTIC APPROXIMATION FOR THE SWITCHING TIME

The switching process consists of two stages. The first stage is the field sweep time interval, $0 < t < \tau_h$. The second stage is the motion in the constant field for the time interval $\tau_h < t < \tau_m$. Below we use two different approximations to find the magnetic dynamics in each stage.

A. First stage

The idea for the first stage approximation is to assume that the deviation of $\mathbf{n}$ from $+z$ is small. The rational for that is provided by the following argument. The initial position of the moment is given by $\theta_u \approx h_\perp/(\omega_0 + h_0) \ll 1$, i.e., is very close to $+z$. We then assume that proximity to the $+z$ holds throughout the first stage if the sweep time is not too long. The precise condition imposed by this assumption on τ_h is not clear at this point but will be obtained after we do the calculations.

According to the above, we linearize the LLG equation near the $+z$ point. In the linearized equation the unknowns are the two projections (n_x, n_y) of the unit vector. Both are small for $\mathbf{n}$ close to $+z$. One gets a linear system

$$\begin{aligned} \dot{n}_x &= -\alpha(\omega_0 + h) n_x - (\omega_0 + h) n_y + \alpha h_\perp \\ \dot{n}_y &= = (\omega_0 + h) n_x - \alpha(\omega_0 + h) n_y - h_\perp \ . \end{aligned}$$

Introducing a notation $\omega(t) = \omega_0 + h(t)$ we rewrite it as

$$\begin{pmatrix} \dot{n}_x \\ \dot{n}_y \end{pmatrix} = \begin{vmatrix} -\alpha\omega(t) & -\omega(t) \\ \omega(t) & -\alpha\omega(t) \end{vmatrix} \begin{pmatrix} n_x \\ n_y \end{pmatrix} + \begin{pmatrix} \alpha h_\perp \\ -h_\perp \end{pmatrix} \quad (7)$$

The matrix on the right hand side can be diagonalized by changing variables to $\xi = n_x + i n_y$, $\eta = n_x - i n_y$. Using them we get two decoupled equations

$$\begin{aligned} \dot{\xi} &= (i - \alpha)\big[\omega(t)\xi - h_\perp\big] \ , \\ \dot{\eta} &= -(i + \alpha)\big[\omega(t)\eta - h_\perp\big] \ , \end{aligned}$$

which turn out to be complex conjugates of each other. Consequently, we can solve either one of them. Denoting $\mu = i - \alpha$, we search for the solution of the first equation in the form

$$\xi(t) = A(t) e^{\mu \int_0^t \omega(s) ds} \ .$$

For future notation we define a phase function $\varphi(t) = \int_0^t \omega(s) ds$. The solution is found to be

$$\xi(t) = \xi(0) e^{\mu\varphi(t)} - \mu h_\perp e^{\mu\varphi(t)} \int_0^t e^{-\mu\varphi(u)} du \ .$$

Going back to (n_x, n_y) we obtain after the necessary algebraic transformations a solution

$$\begin{aligned} n_x &= e^{-\alpha\varphi} \{ n_{x0} \cos\varphi - n_{y0} \sin\varphi - \\ &- h_\perp [(S - \alpha C)] \cos\varphi - (C + \alpha S)] \sin\varphi] \} \ , \\ n_y &= e^{-\alpha\varphi} \{ n_{x0} \sin\varphi + n_{y0} \cos\varphi - \\ &- h_\perp [(S - \alpha C)] \sin\varphi + (C + \alpha S)] \cos\varphi] \} \ , \end{aligned} \quad (8)$$

where we have defined

$$\begin{aligned} S(t) &= \int_0^t e^{\alpha\varphi(s)} \sin\phi(s) ds \ , \quad (9) \\ C(t) &= \int_0^t e^{\alpha\varphi(s)} \cos\phi(s) ds \ . \end{aligned}$$

In our case the initial conditions are given by

$$n_{x0} = \frac{h_\perp}{\omega_0 + h}, \quad n_{y0} = 0 \ , \quad (10)$$

thus both projections n_x and n_y are proportional to $h_\perp$ and we should be able to satisfy the assumption of small deviation from the origin for sufficiently small bias field. Below we will calculate how small should $h_\perp$ be to ensure small deviations in Stage I.

For the linear field sweep (5) the phase $\varphi(t)$ is a quadratic function

$$\varphi = \int_0^t \left(\omega_0 + h_0\left(1 - \frac{2s}{\tau_h}\right)\right) ds = (\omega_0 + h_0)t - h_0\frac{t^2}{\tau_h} \ .$$

In this case the integrals (9) can be found exactly and expressed through the error function of complex argument (Appendix A).

Here we will consider a useful approximation valid in a large region of parameters. The phase $\varphi(t)$ has one maximum on the interval $[0, \tau_h]$ at the point $t_m = \tau_h(\omega_0 + h_0)/2h_0$ (recall that $\omega_0 < h_0$). The presence of a maximum means that the integrals for $C(\tau_h)$ and $S(\tau_h)$ can be approximated by a steepest descent (stationary phase) method in the case of a large change of φ on the integration interval $[0, \tau_h]$. This certainly requires the inequality $\omega_0\tau_h \gg 1$ to hold but, as it turns out below, sometimes an even stronger condition is needed. The steepest descent calculation is performed in Appendix A and gives an approximation

$$\begin{aligned} S &= e^{\alpha\phi_m}\sqrt{\frac{\pi\tau_h}{h_0}}\left[\sin\left(\phi_m - \frac{\pi}{4}\right) + \frac{\alpha}{2}\cos\left(\phi_m - \frac{\pi}{4}\right)\right] \ , \\ C &= e^{\alpha\phi_m}\sqrt{\frac{\pi\tau_h}{h_0}}\left[\cos\left(\phi_m - \frac{\pi}{4}\right) - \frac{\alpha}{2}\sin\left(\phi_m - \frac{\pi}{4}\right)\right] \ , \\ \varphi_m &\equiv \varphi(t_m) = \frac{(\omega_0 + h_0)^2}{4h_0}\tau_h \ . \end{aligned} \tag{11}$$

Substituting this into (8), using $\varphi(\tau_h) = \omega_0\tau_h$ and performing the calculations we find

$$\begin{aligned} n_x(\tau_h) &= e^{-\alpha\omega_0\tau_h}\frac{h_\perp}{\omega_0 + h_0}\cos\omega_0 t - \\ &- e^{\alpha\Delta\varphi}h_\perp\sqrt{\frac{\pi\tau_h}{h_0}}(\sin\overline{\Delta\varphi} - \frac{\alpha}{2}\cos\overline{\Delta\varphi}) \ , \\ n_y(\tau_h) &= e^{-\alpha\omega_0\tau_h}\frac{h_\perp}{\omega_0 + h_0}\sin\omega_0 t - \\ &- e^{\alpha\Delta\varphi}h_\perp\sqrt{\frac{\pi\tau_h}{h_0}}(\cos\overline{\Delta\varphi} + \frac{\alpha}{2}\sin\overline{\Delta\varphi}) \ , \end{aligned} \tag{12}$$

where we have defined

$$\begin{aligned} \Delta\varphi &= \varphi(t_m) - \varphi(\tau_h) = \frac{(\omega_0 - h_0)^2}{4h_0}\tau_h \ , \\ \overline{\Delta\varphi} &= \Delta\varphi - \frac{\pi}{4} \ . \end{aligned} \tag{13}$$

We observe that in both formulae the first term on the right hand side is initially small and further decreases as a function of τ_h, while the second term increases with τ_h. Therefore the condition for small deviations can be formulated as the smallness of the second term

$$e^{\alpha\Delta\varphi}h_\perp\sqrt{\frac{\pi\tau_h}{h_0}} \ll 1 \ .$$

Explicitly separating the product $\omega_0\tau_h$, we can write the condition on the bias field

$$\frac{h_\perp}{\omega_0} \ll \sqrt{\frac{h_0}{\pi\omega_0}}\sqrt{\frac{1}{\omega_0\tau_h}}\exp\left[-\alpha\frac{(\omega_0 - h_0)^2}{4h_0\omega_0}(\omega_0\tau_h)\right] \ , \tag{14}$$

which will guarantee the validity of the small deviations assumption. Additional inequalities (A4) enabling the approximation (11) are listed in Appendix A and have to be satisfied as well. We will return to their discussion in Sec. V.

B. Second Stage

During the Stage II the external magnetic field is constant, $\mathbf{H} = -H_0\hat{z} + H_\perp\hat{x}$. The action of the bias field $H_\perp$ can be viewed as a perturbation of the axially symmetric problem with $H_\perp = 0$ and $H = -H_0$. For the unperturbed problem the switching time is a known[28,29] as a function of θ_{in}, the angular deviation of the magnetization from the easy axis at the beginning of Stage II.

To find the perturbation corrections to the axially symmetric problem we employ the method of deriving an approximate differential equation for the total energy ε in the limit of small Gilbert damping constant (see, e.g., Ref. 30). In the $\alpha \to 0$ limit the motion of the moment $\mathbf{M}(t)$ can be viewed as a fast precession along the $\varepsilon =$ const lines and a slow motion from one equipotential orbit to the next one nearby. Up to the linear terms in α the change of energy upon one precession cycle around an orbit is given by

$$\Delta\varepsilon = -\alpha\oint_\Gamma\left|\frac{\partial\varepsilon}{\partial\mathbf{n}}\right|dn = -\alpha f_1(\varepsilon) \ , \tag{15}$$

and the period of this cycle is

$$T = \oint_\Gamma\frac{dn}{|\partial\varepsilon/\partial\mathbf{n}|} = f_2(\varepsilon) \ , \tag{16}$$

where the integrals are taken along the constant energy orbit $\Gamma(\varepsilon)$ on the unit sphere. In this approximation the differential equation for $\varepsilon(t)$ reads[30]

$$\frac{d\varepsilon}{dt} = \frac{\Delta\varepsilon}{T} = -\alpha\frac{f_1(\varepsilon)}{f_2(\varepsilon)} = -\alpha\psi(\varepsilon) \ . \tag{17}$$

Its solution is given by

$$t = -\frac{1}{\alpha}\int_{\varepsilon_1}^{\varepsilon_2}\frac{d\varepsilon}{\psi(\varepsilon)} \ ,$$

and determines the time required to move from the orbit with energy $\varepsilon = \varepsilon_1$ to the orbit with $\varepsilon = \varepsilon_2$.

To find the integrals (15) and (16), we have to find the orbits $\Gamma(\varepsilon)$. When $h_\perp$ is small, one can expect that the equipotential orbits will be close to those in the unperturbed case with $h_\perp = 0$. The latter are the circles of constant polar angle. Indeed, in the absence of the bias

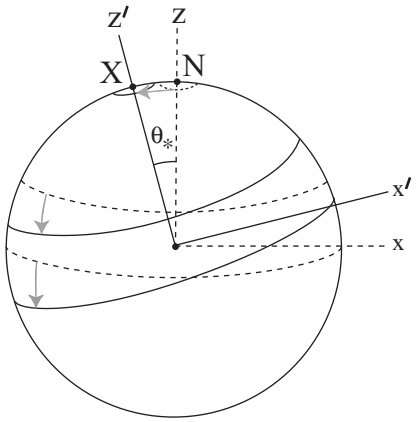

FIG. 3: Rotated reference frame and the definition of θ_*. Unperturbed equipotential orbits are shown in dashed lines and the actual orbits given by the solid lines. Grey arrows show the transformation of the representative orbits as the bias field $h_\perp$ is turned on. Point X is the energy maximum position in the presence of bias field.

field $\varepsilon = \varepsilon_0(\theta)$ and for any given energy the polar angle is given by an inverse function $\theta = \theta_0(\varepsilon)$. This statement is true most of the time, however important exceptions exist. As shown in Fig. 3, the orbits are indeed relatively close near the equator. But near the North pole N of the sphere the orbits of the perturbed energy are small circles around the maximum point X, while the original orbits are small circles around N. They are not relatively close in the sense that the perturbation is larger than the orbit size.

One can remedy the situation by switching to a coordinate system with the z' axis going through the maximum point X. The new coordinate system (x', y', z') is rotated with respect to the original (x, y, z) system by an angle θ_* around the fixed $y' = y$ axis (see Fig. 3). The spherical angles of the new system will be denoted by θ' and ϕ'. The advantage of the rotated system comes form the fact that the perturbed orbits are close to $\theta' = \text{const}$ circles everywhere, except in the vicinity of $\theta' = \pi$. For the region of interest $0 < \theta' \leq \pi/2$ it is possible to define the shape of the orbit $\Gamma(\varepsilon)$ as a perturbation $\theta'(\phi', \varepsilon) = \theta_0(\varepsilon) + h_\perp \delta\theta(\phi', \varepsilon)$ around the circles of constant θ'.

To prove the geometrically intuitive statement of the preceding paragraph one has to invert the equation $\varepsilon(\theta', \phi') = \varepsilon$. The form of energy function in the new spherical angles if calculated in the Appendix B. Up to the first order in $h_\perp$ we find

$$\varepsilon = \varepsilon_0(\theta') + \beta\varepsilon_1(\theta', \phi') + \dots \tag{18}$$

where the small parameter is

$$\beta = \frac{h_\perp}{h_0 - \omega_0} \tag{19}$$

and

$$\begin{aligned} \varepsilon_0(\theta') &= -\frac{\omega_0}{2}\cos^2\theta' + h_0\cos\theta' \\ \varepsilon_1(\theta') &= \omega_0(1-\cos\theta')\sin\theta'\cos\phi' \end{aligned} \tag{20}$$

As expected, the zeroth order term is given by the unperturbed energy as a function of the new polar angle θ'. The same would have happened in the original coordinates, but there is an important difference between the new and original coordinates, which manifests itself in the behavior of ε_1 at small values of θ'. Note that the second term in (18) grows with θ' slower than the first one: $\varepsilon_1 \sim {\theta'}^3$, while $\varepsilon_0 - \varepsilon_0(0) \sim {\theta'}^2$. As a result, the inequality $\beta\varepsilon_1 \ll \varepsilon_0 - \varepsilon_0(0)$ holds uniformly in θ'. We will see in a moment that it is precisely this uniformity that is important. In the original coordinates as $\theta \to 0$ at an arbitrarily small but fixed β the second term exceeds the first one, and the uniformity is violated.

The orbit equation $\theta' = \theta'(\phi', \varepsilon)$ is found form the constant energy condition

$$\varepsilon_0(\theta') + \beta(1-\cos\theta')\sin\theta'\cos\phi' = \varepsilon \ ,$$

which has to be solved for θ'. The solution is searched in the form of a power series in β

$$\theta' = \theta_0(\varepsilon) + \beta\theta_1(\phi', \varepsilon) + \dots$$

where $\theta_0(\varepsilon)$ is the inverse function of $\varepsilon_0(\theta)$, as was already discussed above. Up to the first order in β we find

$$\theta' = \theta_0(\varepsilon) - \beta\frac{\varepsilon_1(\theta_0(\varepsilon), \phi')}{(d\varepsilon_0/d\theta)|_{\theta=\theta_0(\varepsilon)}} + \dots \tag{21}$$

In the "dangerous" limit of small $\theta_0(\varepsilon)$ near the North pole the second term in (21) is proportional to ${\theta_0}^2(\varepsilon)$ thus being a small correction. Due to $\beta \ll 1$ it remains a small correction for the energy values up to near the equator $\varepsilon \approx 0$. This algebraically proves the geometrically intuitive conclusion made above: the perturbed orbits are close to the $\theta' = \text{const}$ lines.

Using the approximations (18) and (21) for the energy and orbit shape, the integrals (15) and (16) can be evaluated up to the first order in β. The details are given in the Appendix C. Substituting the results into Eq. (17) we get a differential equation

$$\frac{d\varepsilon}{dt} = -\alpha\left(\frac{\partial\varepsilon_0}{\partial\theta}\right)^2_{\theta=\theta_0(\varepsilon)} + \ \mathcal{O}(\beta^2) \ . \tag{22}$$

Up to the first order terms in β this is the same equation as one would have for magnetic switching in the unperturbed case with $h_\perp = 0$. We conclude that in the rotated coordinates one can approximate the switching time by the expression for the unperturbed case. The latter[28,29] is reviewed in Appendix D and gives the switching time as a function of the starting angle θ_{in} and the cut-off angle θ_{sw}. To find the time τ_2 spent by the moment in Stage II we just have to set θ_{in} to

be the value of θ' at the end of Stage I, and θ_{sw} to be the value of θ' at the selected switching moment given by $\varepsilon = 0$. Thus $\theta_{in} = \theta'(n_x(\tau_h), n_y(\tau_h))$ and $\theta_{sw} = \theta'(\theta = \pi/2, \phi = \pi/2) = \pi/2$. The substitution is performed in Appendix D and gives

$$\tau_2 = \frac{1}{2\alpha}\left\{\frac{1}{h_0-\omega_0}\ln\left(\frac{h_0-\omega_0\cos\theta_{in}}{h_0(1-\cos\theta_{in})}\right) - \right. \\ \left. - \frac{1}{h_0+\omega_0}\ln\left(\frac{h_0-\omega_0\cos\theta_{in}}{h_0(1+\cos\theta_{in})}\right)\right\} \quad (23)$$

C. Total switching time

The total switching τ_m time is given by the sum of the contributions from Stages I and II and equals $\tau_m = \tau_h + \tau_2$. To use the expression (23) for τ_2 we need the value of θ_{in}. This angle is given by the distance between the endpoint of Stage I $\{n_x(\tau_h), n_y(\tau_h)\}$ and the position of the energy maximum point X given by $(-h_\perp/(h_0-\omega_0), 0)$ on a unit sphere. Since the point $\{n_x(\tau_h), n_y(\tau_h)\}$ and the point X are both close to $+z$, we can approximately write

$$\theta_{in} = \sqrt{(n_x(\tau_h) + h_\perp/(h_0-\omega_0))^2 + n_y(\tau_h)^2} \quad (24)$$

A long expression for θ_{in} can be obtained by substituting the formulae (12) into the equation above.

As it was already discussed, the expressions (12) represent n_x and n_y as a sum of two terms, where the first decreases and the second increases with time. Calculations are substantially simplified when the increasing term dominates, which turns out to be true in a large part of the parameter space. Even for small values of α this is guaranteed for $1/(\omega_0+h_0) \ll \sqrt{\tau_h/h_0}$ or

$$\omega_0\tau_h \gg \frac{\omega_0 h_0}{(\omega_0+h_0)^2} \quad (25)$$

Since we already assumed that $\omega_0\tau_h \gg 1$, and the right hand side of (25) is always less than $1/4$, this inequality is automatically satisfied whenever we can use the steepest descent approximation (12) for Stage I.

Next, we assume that one can also ignore $h_\perp/(h_0-\omega_0)$ in the first term of Eq. (24) compared with $n_x(\tau_h)$ given by the dominant term of (12). This condition is satisfied for $1/(h_0-\omega_0) \ll \sqrt{\tau_h/h_0}$ or

$$\omega_0\tau_h \gg \frac{\omega_0 h_0}{(h_0-\omega_0)^2} \quad (26)$$

As a result, leaving only the dominant terms we obtain

$$\theta_{in} \approx h_\perp\sqrt{\frac{\pi\tau_h}{h_0}}\, e^{\alpha\Delta\varphi} \quad (27)$$

Using the smallness of θ_{in}, we approximate $\sin\theta_{in} \approx \theta_{in}$ and $\cos\theta_{in} \approx 1$ in the expression (23) and rewrite τ_2 as

$$\tau_2 = \frac{1}{2\alpha}\left\{\frac{1}{h_0-\omega_0}\ln\left(\frac{2(h_0-\omega_0)}{h_0\theta_{in}^2}\right) - \right. \\ \left. - \frac{1}{h_0+\omega_0}\ln\left(\frac{h_0-\omega_0}{2h_0}\right)\right\} = \\ = \frac{\ln(1/\theta_{in}^2)}{2\alpha(h_0-\omega_0)} + \tau_R\ , \quad (28)$$

where

$$\tau_R(\alpha, h_0, \omega_0) = \frac{1}{2\alpha}\left\{\frac{1}{h_0-\omega_0}\ln\left(\frac{2(h_0-\omega_0)}{h_0}\right) - \right. \\ \left. - \frac{1}{h_0+\omega_0}\ln\left(\frac{h_0-\omega_0}{2h_0}\right)\right\} \quad (29)$$

is a time interval independent of τ_h and $h_\perp$.

Substituting θ_{in} from Eq. (27) into Eq. (28), we produce the first principal result of our paper, a formula for the switching time

$$\tau_m = \tau_h + \frac{\ln[h_0/\pi h_\perp^2\tau_h] - \alpha\Delta\phi(\tau_h)}{2\alpha(h_0-\omega_0)} + \tau_R \quad (30) \\ = \frac{3h_0+\omega_0}{4h_0}\tau_h + \frac{\ln[h_0/\pi h_\perp^2\tau_h]}{2\alpha(h_0-\omega_0)} + \tau_R(\alpha, h_0, \omega_0)\ .$$

The obtained $\tau_m(\tau_h)$ dependence indeed has a minimum. It is reached at the optimal field sweep time

$$\tau_h^* = \frac{1}{2\alpha(h_0-\omega_0)}\frac{4h_0}{3h_0+\omega_0} \quad (31)$$

that is independent of the bias field. This formula is our second main result. The independence of τ_h^* of $h_\perp$ is a result of the logarithmic dependence in the second term of (30) and ultimately stems from the logarithmic dependence of τ_2 on the initial deviation angle.

The minimal switching time $\tau_m(\tau_h^*)$ corresponding to the optimal field sweep time equals to

$$\tau_m(\tau_h^*) = \frac{1+\ln\left(\frac{\alpha(h_0-\omega_0)(3h_0+\omega_0)}{2\pi h_\perp^2}\right)}{2\alpha(h_0-\omega_0)} + \tau_R\ .$$

It does depend on $h_\perp$, which is a quite natural since the initial deviation from the easy axis is controlled by the bias field.

Expression (30) has its limits of applicability discussed in the next section. In particular, it is not applicable for small τ_h where the steepest descent approximation (11) is invalid. Nevertheless, one can easily calculate $\tau_m(0)$ since in this case there is no motion in Stage I, and, according to Figs. 1 and 3, the initial angle for Stage II is simply

$$\theta_{in} = \theta_u + \theta_* = \frac{h_\perp}{h_0+\omega_0} + \frac{h_\perp}{h_0-\omega_0}\ .$$

Using this value of θ_{in} in (28) we get

$$\tau_m(0) = \frac{1}{\alpha(h_0-\omega_0)}\ln\left(\frac{h_0^2-\omega_0^2}{2h_0h_\perp}\right) + \tau_R\ . \quad (32)$$

The drop of switching time from $\tau_h = 0$ to the minimal value is given by a formula

$$\tau_m(0) - \tau_m(\tau_h^*) = \frac{\ln\left(\frac{\pi(h_0-\omega_0)(h_0+\omega_0)^2}{2\alpha h_0^2(3h_0+\omega_0)}\right) - 1}{2\alpha(h_0-\omega_0)} \ .$$

Note that this difference is again independent of the bias field $h_\perp$, as long as the approximation (30) is valid. The fractional change $(\tau_m(0) - \tau_m(\tau_h^*))/\tau_m(0)$ will depend on the bias field, being an increasing function of $h_\perp$.

V. VALIDITY REGIONS OF THE ANALYTIC APPROXIMATION

A number of approximations were made in our derivation and the final expressions can only be used in the region on their validity.

The approximations made in our treatment of Stage I are as follows.

(a) The steepest descent method employed to evaluate the integrals (9) has to be sufficiently accurate. The required conditions (see (A4) in Appendix A) read

$$\sqrt{\frac{\tau_h}{h_0}} \gg \frac{1}{h_0-\omega_0} > \frac{1}{h_0+\omega_0} \ , \qquad (33)$$

where the second inequality holds automatically.

(b) Next, we assumed that the inequality

$$\frac{h_\perp}{h_0+\omega_0} \ll h_\perp\sqrt{\frac{\pi\tau_h}{h_0}}$$

is satisfied, allowing one to neglect the first terms on the right hand sides of Eqs. (12). However, this requirement is not new because it is already contained in (33).

(c) In order to make approximations in Eq. (24) we required the inequality (25) to hold. This inequality is also contained in (33) and does not add new conditions.

(d) Finally, the inequality (14) should be satisfied to ensure small deviation of $\mathbf{n}$ from $+z$.

Overall, the inequalities

$$\frac{h_\perp}{h_0-\omega_0} \ll h_\perp\sqrt{\frac{\tau_h}{h_0}} \ll e^{-\alpha\Delta\varphi(\tau_h)} < 1 \qquad (34)$$

summarize the requirements for Stage I. For our treatment of Stage II we assumed the following.

(e) The Gilbert damping constant should be small, $\alpha \ll 1$, to be able to use the orbit averaged equation of motion (17).

(f) The parameter describing the orbit deformation (21) should be small, $\beta = h_\perp/(h_0-\omega_0) \ll 1$. But this inequality follows from (34) and thus brings no additional restrictions.

The requirements (34) discussed above can be equivalently presented as conditions on τ_h that have to be satisfied at fixed bias field $h_\perp$. In this form they read

$$\frac{h_0}{(h_0-\omega_0)^2} \ll \tau_h \ll \tau_h^{(+)} \ , \qquad (35)$$

where $\tau_h^{(+)}$ is a solution of

$$\sqrt{\frac{\tau_h}{h_0}}e^{-\alpha\Delta\varphi(\tau_h)} = \frac{1}{h_\perp} \ .$$

We can now check when does the optimal field sweep time τ_h^* lie in the region of validity of our approximation. Using our result (31) we can write

$$\tau_h^* \approx \frac{1}{2\alpha(h_0-\omega_0)} \ ,$$

and substitute it into the requirement (33). We get

$$\alpha \ll \frac{h_0-\omega_0}{2h_0} \ .$$

The right hand side of this inequality is always smaller than unity, thus it automatically implies $\alpha \ll 1$.

We also have to satisfy the condition (14) at $\tau_h = \tau_h^*$. For the exponent $\alpha\Delta\phi$ one can write

$$\alpha\Delta\varphi(\tau_h^*) = \alpha\frac{(h_0-\omega_0)^2}{4h_0}\tau_h^* \approx \frac{h_0-\omega_0}{8h_0} \le \frac{1}{8} \ll 1 \ ,$$

and thus condition (14) simplifies to

$$h_\perp\sqrt{\frac{\tau_h^*}{h_0}} \ll 1$$

The above inequalities on α and $h_\perp$ can be combined into a single requirement

$$\frac{h_\perp^2}{h_0(h_0-\omega_0)} \ll \alpha \ll \frac{h_0-\omega_0}{2h_0} \ . \qquad (36)$$

If the inequalities (36) are satisfied, the optimal sweep time τ_h^* occurs inside the interval (35) and can be calculated using the formula (31).

VI. COMPARISON OF ANALYTIC AND NUMERIC RESULTS

Comparisons of the analytic approximation and exact numeric results were performed in Ref. 2 and shown a very good agreement between the two.

First, we compared the numerically calculated switching times with the expression (30). When the inequalities (36) were well satisfied, the quality of approximation was very good (Fig. 4). As one approached the limits of the approximation's validity by, e.g., increasing α, the errors grew larger.

Second, the numeric results for optimal field sweep time τ_h^* were compared with the formula (31). The correspondence was generally good (Fig. 5), although some visible deviations existed. They were attributed to the fact that the accuracy of the determination of τ_h^* is lowered by a flat shape of the $\tau_m(\tau_h)$ curve minimum. Because of the shallow minimum, small errors in τ_m produce much larger errors in τ_h^*.

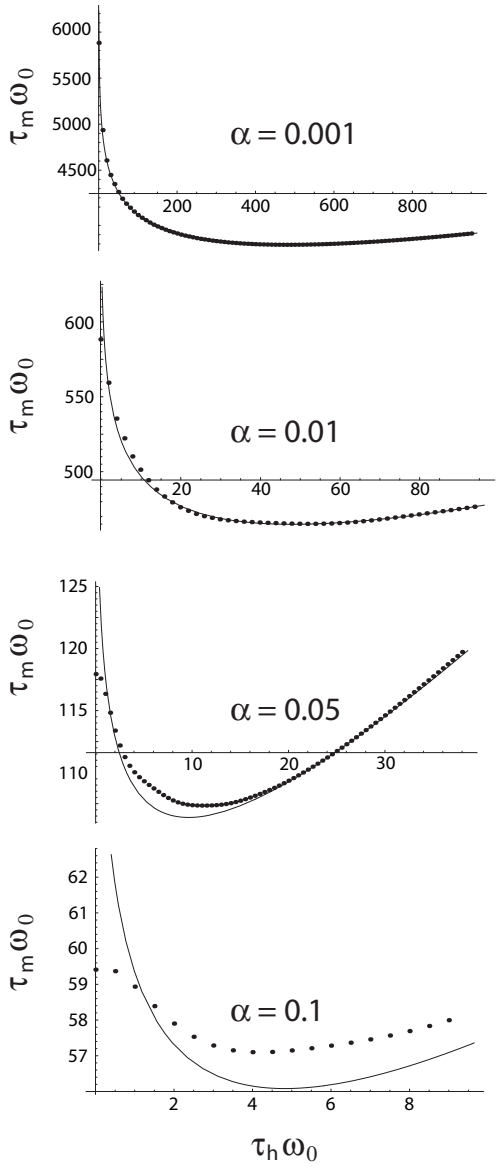

FIG. 4: Dependencies $\tau_m(\tau_h)$ calculated for $h_0 = 2.2\ \omega_0$, $h_\perp = 0.001\ \omega_0$, and variable α indicated on each panel. As α increases, the theoretical fit gets poorer due to the violation of the strong inequality (36).

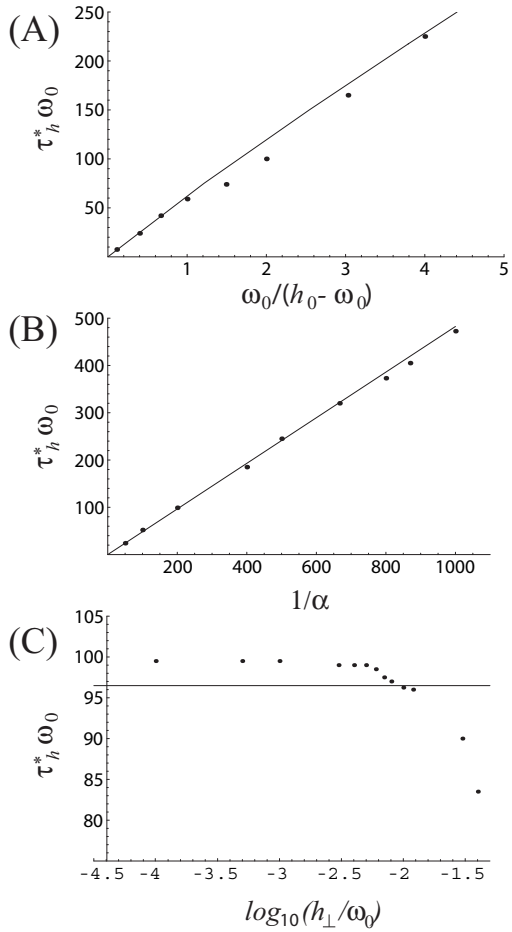

FIG. 5: Numeric (points) and approximate analytical (solid lines) dependencies of the optimal field sweep time τ_h^* on the system parameters. (A) fixed α and $h_\perp$, (B) fixed h_0/ω_0 and $h_\perp$, (C) fixed h_0/ω_0 and α. When not varied, the parameter values are $h_0 = 2.2\omega_0$, $\alpha = 0.01$, $h_\perp = 0.005$.

In general, the analytic expression approximated the $\tau_m(\tau_h)$ dependence up to a 10% accuracy in a surprisingly wide range of parameters. Such accuracy is certainly sufficient for the estimates related to the device design.

When τ_h is outside of the validity region of the results (30) and (31), exact expressions (9) and (24) for the integrals and the initial angle θ_{in} can be used. As long as the deviation from the $+z$ direction in Stage I remains small, they provide a good approximation for τ_m. Consider for example the case of small τ_h. Approximation (30) does not work for $\tau_h \to 0$ predicting an infinite increase of τ_m, while the actual limit $\tau_m(0)$ is finite and given by formula (32). It was checked that using the exact expressions (A3) for the integrals C and S and the formula (24) for θ_{in}, one can obtain an excellent agreement between the two-stage theory and the no-approximation numeric simulations in this limit.

VII. PHYSICAL PICTURE OF THE BALLISTIC-ASSISTED SWITCHING

We now discuss the physical reason for the minimum of the function $\tau_m(\tau_h)$ which was identified in Ref. 2 as the contribution of ballistic switching. We start by noticing that the bias field has two roles in the switching process. First, it provides the initial deviation from the easy axis. Second, it alters the equations of motion for $\mathbf{n}(t)$. The first role of $h_\perp$ manifests itself in our formulae in two ways: by providing the first terms in expressions (12) and by introducing the term $h_\perp/(h_0 - \omega_0)$ into the formula (24). In our derivation of the switching time expression (30) we have found that both contributions are negligible.

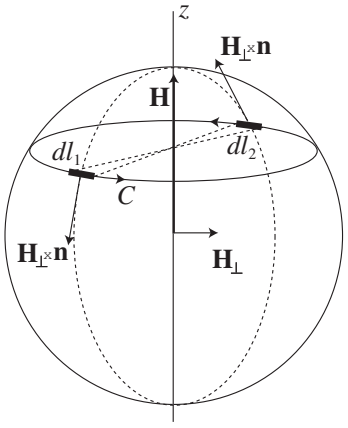

FIG. 6: Average ballistic contribution of the bias field. Vector $\mathbf{n}(t)$ orbits around a parallel circle C on a unit sphere. The torque due to $h_\perp$ pushes $\mathbf{n}$ along the meridians of the sphere. In constant switching field the torque contributions from the diametrically opposed elements dl_1 and dl_2 cancel each other. For variable $\mathbf{H}(t)$ the cancelation does not happen (see text).

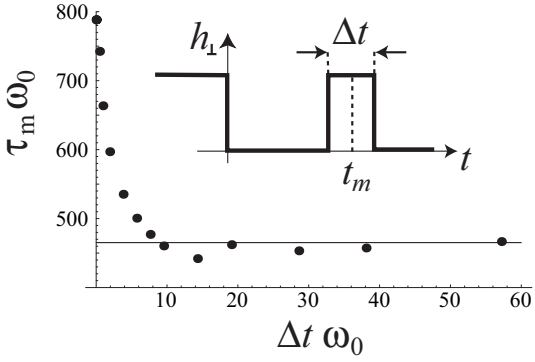

FIG. 7: Numerically calculated witching time with pulsed bias field. The parameters are set to $h_0 = 2.2\omega_0$, $h_\perp = 0.001\omega_0$, $\alpha = 0.01$ (cf. Fig. 4). Field sweep time is fixed at $\tau_h = 50/\omega_0$, close to the optimal sweep time $\tau_h^* = 48.2/\omega_0$. The time dependence of the pulsed bias field $h_\perp(t)$ is shown in the inset. As the width of the pulse Δt approaches the theoretical target of $2\sqrt{\tau_h/h_0} \approx 10/\omega_0$, the switching time approaches the value obtained at $h_\perp = \text{const}$ (shown by a horizontal line).

Therefore within our approximation only the second role of the bias field is important.

Let us proceed by discussing this role qualitatively. Recall that in the absence of anisotropy and other fields the torque $\mathbf{H}_\perp \times M_0\mathbf{n}$ due to the bias field would rotate the unit vector $\mathbf{n}$ from $+z$ to $-z$ along a meridian of the unit sphere (dashed line in Fig. 6), in a "ballistic" or "precessional" fashion. In our case a weak bias field is applied on top of the strong uniaxial anisotropy and switching field, which induce a fast orbital motion of vector $\mathbf{n}(t)$ along the parallel circles (line C in Fig. 6). The bias field still attempts to move $\mathbf{n}$ along the meridians, but now its action has to be averaged over the period of orbital motion. As illustrated in Fig. 6, in constant fields $\mathbf{H}||\hat{z}$ averaging gives zero due to the cancelation of the contributions from the diametrically opposed infinitesimal intervals dl_1 and dl_2 of equal lengths. This way ballistic contribution of the bias field is quenched. However, the contribution of $\mathbf{H}_\perp$ does not average to zero for a variable switching field $\mathbf{H}(t)$. In this case the velocity of $\mathbf{n}$ changes along the orbit, the times spent in the intervals dl_1 and dl_2 are different, and the contributions of the two do not cancel each other. We conclude that in the presence of a time dependent field $\mathbf{H}(t)$ ballistic contribution of the perpendicular bias field is partially recovered.

Based on the discussion above, we may expect to find that the largest contribution of the ballistic switching will happen when the change of velocity is biggest. The measure of the velocity change is $\Delta\omega/\omega$, where $\Delta\omega$ is the change of the velocity as one precesses from the interval dl_1 to the interval dl_2. We may estimate

$$\frac{\Delta\omega}{\omega} \sim \frac{\dot{\omega}T}{\omega} \sim \frac{\dot{\omega}}{\omega^2} \sim \frac{\ddot{\phi}}{\dot{\phi}^2}\,,$$

where $T = 2\pi/\omega$ is the instantaneous period. We see that the velocity change estimate diverges at the point $\dot{\phi} = 0$. But this is exactly the stationary phase point t_m that gives the largest contribution to the integrals (9) in our approximation. We have thus established a one-to-one correspondence between the qualitative description of the ballistic contribution and our derivation of the analytic approximation (30). To illustrate the fact that the action of $h_\perp$ is only important near the stationary phase point t_m, we have performed a numeric experiment with pulsed bias field $h_\perp(t)$ changing in time as shown in the inset of Fig. 7. It is kept constant for $t < 0$, switched off at $t = 0$, and then switched on again for a short interval of time Δt, centered around the t_m point. With the pulsed bias field the ballistic contribution is only present during the interval Δt. It follows from the steepest descent calculation of Appendix A that formulae (11) would be valid already for $\Delta t \gtrsim 2\sqrt{\tau_h/h_0}$, and when this inequality is satisfied our theory would predict the same switching time (30) for pulsed and constant bias fields. The results of the numeric experiment (Fig. 7) are completely consistent with this prediction. As the pulse width approaches the value of $2\sqrt{\tau_h/h_0}$, the switching time drops to the value obtained earlier at constant $h_\perp$.

The minimum of the $\tau_m(\tau_h)$ function can be understood as follows. Ballistic contribution helps to move vector $\mathbf{n}$ from $+z$ to $-z$ and is thus responsible for the initial decrease of τ_m. As the sweep time grows larger, the change of the orbital velocity during the precession period decreases and the ballistic contribution averages out progressively better. The helping effect of ballistic switching is lost and τ_m starts to increase as it normally would.

Finally, we want to remark that ballistic contribution to switching can be also viewed as a phenomenon complimentary to the magnetic resonance and RF-assisted switching.[21–27] In the case of RF-field application the ex-

ternal field $\mathbf{H}$ is constant, while the bias field $\mathbf{H}_\perp(t)$ is time-dependent. Here the contributions of the bias field torque on the intervals dl_1 and dl_2 in Fig. 6 do not cancel each other because the torque itself changes with time. This, again, leads to a nonzero average of the bias field contribution on a precession orbit and creates a helping effect for the magnetic switching process. From this point of view the magnetic resonance and the time dependence of the axial switching field are two different ways to achieve the same goal: a non-vanishing average contribution of the bias field torque on an orbit.

VIII. CONCLUSIONS

We have identified and investigated the phenomenon of ballistic contribution to the conventional magnetic switching by a time-dependent field. An analytic approximation is derived for the ballistic-assisted switching time in a constant perpendicular bias field. It is also shown that, if practical, a constant bias can be substituted by short pulse of bias field applied near the stationary phase time point. Our results provide a convenient approximation for the optimal field sweep time, an important parameter in the device design. The expressions obtained in this study can be used as a starting point for the investigations of the switching time in granular media, where each grain can be modeled by a single moment and bias field is produced by the other grains or by the spread of grain orientations.

IX. ACKNOWLEDGMENTS

Ya. B. Bazaliy is grateful to B. V. Bazaliy for illuminating discussions. This work was supported by the NSF grant DMR-0847159.

Appendix A: Steepest descent approximation for $C(t)$ and $S(t)$

Here we evaluate the integrals (9)

$$\begin{aligned} S(\tau_h) &= \int_0^{\tau_h} e^{\alpha\varphi(t)} \sin\varphi(t) dt \\ C(\tau_h) &= \int_0^{\tau_h} e^{\alpha\varphi(t)} \cos\varphi(t) dt \end{aligned}$$

with the phase $\varphi(t)$ given by a real quadratic function

$$\varphi = (\omega_0 + h_0)t - h_0 \frac{t^2}{\tau_h} \ .$$

The integrals in question can be obtained from the real and imaginary parts of a complex integral

$$\begin{aligned} I &= \int_0^{\tau_h} e^{-\mu\varphi(t)} dt = C - iS \ , \qquad \text{(A1)} \\ \mu &= i - \alpha \ . \end{aligned}$$

By completing the square we can rewrite

$$\varphi(t) = \frac{(h_0+\omega_0)^2}{4h_0}\tau_h - \frac{h_0}{\tau_h}(t-t_m)^2 \ ,$$

where $t_m = \tau_h(\omega_0 + h_0)/2h_0$ is the point of maximum phase, $0 < t_m < \tau_h$. Now

$$\begin{aligned} I &= e^{\mu\frac{(h_0+\omega_0)^2}{4h_0}\tau_h} \cdot J \ , \qquad \text{(A2)} \\ J &= \int_0^{\tau_h} e^{-\mu(h_0/\tau_h)(t-t_m)^2} dt \ . \end{aligned}$$

Changing variables to $z = \sqrt{\mu h_0/\tau_h}(t - t_m)$, we can write down J as

$$J = \sqrt{\frac{\tau_h}{\mu h_0}} \int_\Gamma e^{-z^2} dz \ ,$$

where Γ is a straight line in the complex plane going between the points $z_1 = -\sqrt{\mu h_0/\tau_h}\ t_m$ and $z_2 = \sqrt{\mu h_0/\tau_h}\ (\tau_h - t_m)$. Due to our definition of z, line Γ crosses the complex zero point.

Since the integrand of J is a regular function, integration can be performed along any contour connecting z_1 and z_2. The integral can be expressed in terms of the error function of complex variable $\mathrm{Erf}(z) = (2/\sqrt{\pi}) \int_0^z \exp(-z^2) dz$ as[31]

$$J = \sqrt{\frac{\tau_h}{\mu h_0}} \frac{\sqrt{\pi}}{2} \left(\mathrm{Erf}(z_1) + \mathrm{Erf}(z_2)\right) \qquad \text{(A3)}$$

The above in an exact formula. The steepest descent approximation corresponds to the case of large absolute values $|z_1| \gg 1$, $|z_2| \gg 1$. Due to the smallness of α one has $|\mu| \approx 1$, so these conditions translate to

$$\sqrt{\frac{h_0}{\tau_h}} t_m \gg 1 \ , \quad \sqrt{\frac{h_0}{\tau_h}}(\tau_h - t_m) \gg 1 \ ,$$

or equivalently

$$\frac{(h_0+\omega_0)^2}{4h_0}\tau_h \gg 1 \ , \quad \frac{(h_0-\omega_0)^2}{4h_0}\tau_h \gg 1 \qquad \text{(A4)}$$

Using[31] $\mathrm{Erf}(z) \to 1$ for $|z| \to \infty$ we find the approximation

$$J \approx \sqrt{\frac{\pi\tau_h}{\mu h_0}} \approx \sqrt{\frac{\pi\tau_h}{h_0}} e^{i\pi/4} \left(1 - \frac{i\alpha}{2}\right) \ ,$$

where we have also expanded in small α. Substituting this back into (A2) we get

$$I \approx e^{\alpha\varphi_m} \sqrt{\frac{\pi\tau_h}{h_0}} e^{i(\pi/4 - \varphi_m)} \left(1 - \frac{i\alpha}{2}\right) \qquad \text{(A5)}$$

where $\varphi_m = \varphi(t_m)$. The real and imaginary parts of I give C and S according to Eq. (A1)

$$\begin{aligned} C &\approx e^{\alpha\phi_m} \sqrt{\frac{\pi\tau_h}{h_0}} \left[\cos\left(\phi_m - \frac{\pi}{4}\right) - \frac{\alpha}{2}\sin\left(\phi_m - \frac{\pi}{4}\right)\right] \ , \\ S &\approx e^{\alpha\phi_m} \sqrt{\frac{\pi\tau_h}{h_0}} \left[\sin\left(\phi_m - \frac{\pi}{4}\right) + \frac{\alpha}{2}\cos\left(\phi_m - \frac{\pi}{4}\right)\right] \ . \end{aligned}$$

Appendix B: Energy in rotated coordinates

The relationship between the projections of $\mathbf{n}$ and $\mathbf{h}$ in the primed and original coordinate system are given as

$$\begin{aligned} n_z &= n'_z\cos\theta_* + n'_x\sin\theta_* \\ &= \cos\theta'\cos\theta_* + \sin\theta'\cos\phi'\sin\theta_* \\ n_x &= -n'_z\sin\theta_* + n'_x\cos\theta_* = \\ &= -\cos\theta'\sin\theta_* + \sin\theta'\cos\phi'\cos\theta_* \\ n_y &= n'_y \end{aligned}$$

and

$$\begin{aligned} h'_z &= h\cos\theta_* - h_\perp\sin\theta_* \\ h'_x &= h\sin\theta_* + h_\perp\cos\theta_* \end{aligned}$$

One can now rewrite Eq. (4) through the angles (θ', ϕ')

$$\begin{aligned} \varepsilon &= -\frac{\omega_0}{2}{n'_z}^2 - n'_x h'_x - n'_z h'_z = \\ &= -\frac{\omega_0}{2}(\cos\theta'\cos\theta_* + \sin\theta'\cos\phi'\sin\theta_*)^2 \\ &\quad -h(\cos\theta'\cos\theta_* + \sin\theta'\cos\phi'\sin\theta_*) \\ &\quad -h_\perp(\sin\theta'\cos\phi'\cos\theta_* - \cos\theta'\sin\theta_*) \end{aligned} \tag{B1}$$

The above is the exact expression. We are looking at the case $h = -h_0$ and $h_\perp \to 0$. Up to the first order in $h_\perp$

$$\sin\theta_* \approx \frac{h_\perp}{h_0 - K}, \quad \cos\theta_* \approx 1\ .$$

Expanding the energy up to the first order in $h_\perp$ we get

$$\varepsilon \approx \varepsilon_0(\theta') + \beta\varepsilon_1(\theta', \phi') \tag{B2}$$

where the small parameter is

$$\beta = \frac{h_\perp}{h_0 - \omega_0} \tag{B3}$$

and

$$\begin{aligned} \varepsilon_0(\theta') &= -\frac{\omega_0}{2}\cos^2\theta' + h_0\cos\theta' \\ \varepsilon_1(\theta') &= \omega_0(1-\cos\theta')\sin\theta'\cos\phi' \end{aligned} \tag{B4}$$

The first term in the expansion (18) is the energy unperturbed by the bias field, evaluated at the new polar angle θ'.

Appendix C: Integrals along the perturbed orbits

First, we calculate the approximate value of $|\partial\varepsilon/\partial\mathbf{n}|$. Taking the identity

$$\left|\frac{\partial\varepsilon}{\partial\mathbf{n}}\right| = \sqrt{\left(\frac{\partial\varepsilon}{\partial\theta'}\right)^2 + \frac{1}{\sin^2\theta'}\left(\frac{\partial\varepsilon}{\partial\phi'}\right)^2}$$

and expanding in small β up to the first order we find

$$\left|\frac{\partial\varepsilon}{\partial\mathbf{n}}\right| = \frac{\partial\varepsilon_0}{\partial\theta'} + \beta\frac{\partial\varepsilon_1}{\partial\theta'} + \dots \tag{C1}$$

Next, we need the element of orbit length $|dn|$. Using $|dn| = \sqrt{\sin^2\theta d\phi'^2 + d\theta'^2}$ and calculating up to the first order in β we get

$$|dn| = \left(\sin\theta_0 - \beta\frac{\cos\theta_0\ \varepsilon_1(\theta_0,\phi')}{(d\varepsilon_0/d\theta)|_{\theta=\theta_0(\varepsilon)}}\right)d\phi' \tag{C2}$$

Using the form of ε_1 (B4) we will rewrite it as

$$|dn| = (\sin\theta_0 - \beta A(\varepsilon)\cos\phi')\,d\phi'$$

We will further use a notation

$$\varepsilon_1(\theta_0(\varepsilon), \phi') = B(\varepsilon)\cos\phi'$$

To perform the integrals (15) and (16) we use the expansions (C1) and (C2), and, expanding up to the first order in β, get

$$\begin{aligned} \oint_\Gamma \left|\frac{\partial E}{\partial\mathbf{n}}\right| dn &= \int_0^{2\pi}\left[\frac{\partial\varepsilon_0}{\partial\theta}\sin\theta_0 + \right. \\ &+ \left.\beta\left(\frac{\partial B}{\partial\theta}\sin\theta_0 - \frac{\partial\varepsilon_0}{\partial\theta}A\right)\cos\phi' + \dots\right]d\phi' \end{aligned}$$

The integral of first order term in β vanishes and we get

$$\oint_\Gamma \left|\frac{\partial E}{\partial\mathbf{n}}\right| dn = 2\pi\frac{\partial\varepsilon_0}{\partial\theta}\sin\theta_0 + \mathcal{O}(\beta^2)$$

Perform a similar calculation for the integral (16) we get

$$\oint_\Gamma \frac{dn}{|\partial\varepsilon/\partial\mathbf{n}|} = 2\pi\frac{\sin\theta_0}{\partial\varepsilon_0/\partial\theta} + \mathcal{O}(\beta^2)$$

According to (17) the differential equation on $\varepsilon(t)$ reads

$$\frac{d\varepsilon}{dt} = -\alpha\left(\frac{\partial\varepsilon_0}{\partial\theta}\right)^2\Bigg|_{\theta=\theta_0(\varepsilon)} + \mathcal{O}(\beta^2) \tag{C3}$$

Appendix D: Switching time in the unperturbed case

The problem of switching time of a uniaxial particle in the absence of perpendicular field was probably first solved by Kikuchi[28] for the case of $H_z = 0$. The derivation was generalized to arbitrary H_z by many authors, in particular in the appendix of Ref. 29. Here we re-derive this result for the completeness of the presentation. In the case of $h_\perp = 0$ one can find the switching time either by solving Eq. (22) (same as Eq. (C3)) truncated to zeroth order, or by a direct inspection of the system (2), (3). Since ε_0 depends only on θ, it is enough to consider the first equation which reads

$$\dot\theta = -\alpha\frac{\partial\varepsilon}{\partial\theta} = -\alpha(\omega_0\cos\theta + h)\sin\theta$$

Integrating we get

$$-\alpha t = \int_{\theta_{in}}^{\theta_{sw}} \frac{d\theta}{\sin\theta(\omega_0\cos\theta + h)} \ .$$

A variable change $x = \cos\theta$ gives

$$\begin{aligned} t &= \frac{1}{\alpha}\int_{x_{in}}^{x_{sw}} \frac{dx}{(1-x^2)(\omega_0 x + h)} = \\ &= -\frac{1}{2\alpha}\left\{\frac{1}{h+\omega_0}\ln\left(\frac{1-x}{\omega_0 x + h}\right) - \right. \\ &\quad \left. - \frac{1}{h-\omega_0}\ln\left(\frac{1+x}{\omega_0 x + h}\right)\right\}\Bigg|_{x_{in}}^{x_{sw}} \end{aligned} \qquad \text{(D1)}$$

In application to our problem $\theta_{sw} = \pi/2$ ($x_{sw} = 0$) and $h = -h_0$ which gives

$$\begin{aligned} t &= \frac{1}{2\alpha}\left\{\frac{1}{h_0-\omega_0}\ln\left(\frac{h_0 - \omega_0\cos\theta_{in}}{h_0(1-\cos\theta_{in})}\right) - \right. \\ &\quad \left. - \frac{1}{h_0+\omega_0}\ln\left(\frac{h_0 - \omega_0\cos\theta_{in}}{h_0(1+\cos\theta_{in})}\right)\right\} \end{aligned} \qquad \text{(D2)}$$

* Electronic address: yar@physics.sc.edu

1. A. Stankiewicz, APS March Meeting, Portland, OR, March 15-19, 2010, Bulletin of the APS, vol. 55 (2), abstract H33.11.
2. Ya. B. Bazaliy and A. Stankiewicz, Appl. Phys. Lett. **98** 142501 (2011).
3. J. C. Slonczewski, IBM Research Memorandum No. 003.111.224 (1956). Also see L. D. Landau and E. M. Lifshitz, *Electrodynamics of Continuous Media* (Pergamon, New York, 1960), Sec. 37, pp. 150 - 151.
4. Z. Z. Sun and X. R. Wang, Phys. Rev. B **73**, 092416 (2006).
5. A. Sukhov and J. Berakdar, Phys. Rev. Lett. **102**, 057204 (2009).
6. A. Sukhov and J. Berakdar, Applied Physics A **98**, 837 (2010).
7. The case of infinitesimally slow field change can be viewed as the limit of the infinitesimally small jump with $\mathbf{H}_f \to \mathbf{H}_i$ performed at the astroid boundary. The switching time then depends on just one parameter $\mathbf{H}_i$.
8. L. He, W. D. Doyle, and H. Fujiwara, IEEE Trans. Magn. **30**, 4086 (1994).
9. L. He, W. D. Doyle, L. Varga, H. Fujiwara, and P. J. Flanders, J. Magn.Magn. Mater. **155**, 6 (1996).
10. D. G. Porter, IEEE Trans. Magn. **34**, 1663 (1998).
11. M. d'Aquino, D. Suess, T. Schrefl, C. Serpico, and J. Fidler, J. Magn. Magn. Mater. **290-291**, 906 (2005).
12. D. Suess, T. Schrefl, W. Scholz, and J. Fidler, J. Magn. Magn. Mater. **242-245**, 426 (2002).
13. M. Bauer, J. Fassbender, B. Hillebrands, and R. L. Stamps, Phys. Rev. B **61**, 3410 (2000).
14. D. Xiao, M. Tsoi, and Q. Niu, cond-mat/0409671 (2004); J. Appl. Phys. **99**, 013903 (2006).
15. Z. Z. Sun and X. R. Wang, Phys. Rev. B **71**, 174430 (2005).
16. X. R. Wang and Z. Z. Sun, Phys. Rev. Lett. **98**, 077201 (2007).
17. P. P. Horley, V. R. Vieira, P. Gorley, J. G. Hernandez, V. K. Dugaev, and J. Barnas, J. Phys. D **42**, 245007 (2009)
18. C. H. Back, R. Allenspach, W. Weber, S. S. P. Parkin, D. Weller, E. L. Garwin, and H. C. Siegmann, Science **285**, 864 (1999).
19. Th. Gerrits, H. A. M. van den Berg, J. Hohlfeld, L. Bar, and Th. Rasing, Nature **418**, 509 (2002).
20. I. Tudosa, C. Stamm, A. B. Kashuba, F. King, H. C. Siegmann, J. Stohr, G. Ju, B. Lu, and D. Weller, Nature **428**, 831 (2004).
21. C. Thirion, W. Wernsdorfer, and D. Mailly, Nat. Mater. **2**, 524 (2003).
22. W. T. Coffey, D. S. F. Crothers, J. L. Dormann, Yu. P. Kalmykov, E. C. Kennedy, and W. Wernsdorfer, Phys. Rev. Lett. **80**, 5655 (1998).
23. J. L. Garca-Palacios and F. J. Lazaro, Phys. Rev. B **58**, 14937 (1998).
24. G. Bertotti, C. Serpico, and I. D. Mayergoyz, PRL **86**,724 (2001).
25. K. Rivkin, J. B. Ketterson, APL **89**, 252507 (2006).
26. Z. Z. Sun and X. R. Wang, Phys. Rev. B **74** 132401 (2006).
27. W. Scholz, T. M. Crawford, G. J. Parker, T. W. Clinton, T. Ambrose, S. Kaka, and S. Batra, IEEE Trans. Magn. **44**, 3134 (2008).
28. R. Kikuchi, J. Appl. Phys. **27**, 1352 (1956).
29. Y. Uesaka, H. Endo, T. Takahashi, Y. Nakatani, N. Hayashi, and F. Fukushima, Phys. Stat. Solidi **189**, 1023 (2002).
30. R. Bonin, C. Serpico, G. Bertotti, I. D. Mayergoyz, and M. dAquino, Eur. Phys. J. B **59**, 435 (2007).
31. M. Abramovitz, I. Stegun, *Hadbook of Mathematical Functions* (Dover, New York, 1972), Chapter 7.